Controlled Swapping of Nanocomposite Surface Wettability by Multilayer Photopolymerization

7 AUTHORS, INCLUDING:

Francesca Villafiorita-Monteleone
Italian National Research Council
16 PUBLICATIONS   **49** CITATIONS

Claudio Canale
Istituto Italiano di Tecnologia
49 PUBLICATIONS   **823** CITATIONS

Davide Cozzoli
Università del Salento
137 PUBLICATIONS   **5,734** CITATIONS

Despina Fragouli
Istituto Italiano di Tecnologia
75 PUBLICATIONS   **630** CITATIONS

Controlled Swapping of Nanocomposite Surface Wettability by Multilayer Photopolymerization

Francesca Villafiorita-Monteleone,*,[†,‡] Claudio Canale,[§] Gianvito Caputo,[‡] P. Davide Cozzoli,[‡,⊥] Roberto Cingolani,[§] Despina Fragouli,[†] and Athanassia Athanassiou*,[†,‡,§]

[†]Center for Biomolecular Nanotechnologies @UNILE, Istituto Italiano di Tecnologia, via Barsanti, Arnesano, 73100 Lecce, Italy

[‡]National Nanotechnology Laboratory (NNL), CNR - Istituto Nanoscienze, via per Arnesano, 73100 Lecce, Italy

[§]Istituto Italiano di Tecnologia (IIT), via Morego 30, 16163 Genova, Italy

[⊥]Dipartimento di Ingegneria dell'Innovazione, Università del Salento, via per Arnesano, 73100 Lecce, Italy

Ⓢ Supporting Information

ABSTRACT: Single-layered photopolymerized nanocomposite films of polystyrene and TiO_2 nanorods change their wetting characteristics from hydrophobic to hydrophilic when deposited on substrates with decreasing hydrophilicity. Interestingly, the addition of a second photopolymerized layer causes a swapping in the wettability, so that the final samples result converted from hydrophobic to hydrophilic or vice versa. The wettability characteristics continue to be swapped as the number of photopolymerized layers increases. In fact, odd-layered samples show the same wetting behavior as single-layered ones, while even-layered samples have the same surface characteristics as double-layered ones. Analytical surface studies demonstrate that all samples, independently of the number of layers, have similar low roughness, and that the wettability swap is due to the different concentration of the nanocomposites constituents on the samples surface. Particularly, the different interactions between the hydrophilic TiO_2 nanorods and the underlying layer lead to different amounts of nanorods exposed on the nanocomposites surface. Moreover, due to the unique property of TiO_2 to reversibly increase its wettability upon UV irradiation and subsequent storage, the wetting characteristics of the multilayered nanocomposites can be tuned in a reversible manner. In this way, a combination of substrate, number of photopolymerized layers, and external UV light stimulus can be used in order to precisely control the surface wettability properties of nanocomposite films, opening the way to a vast number of potential applications in microfluidics, protein assays, and cell growth.
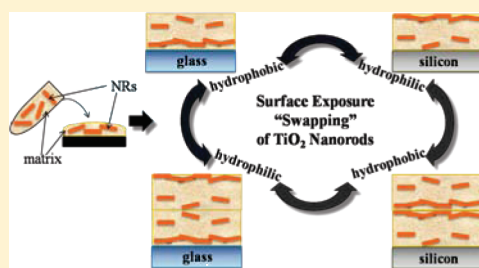
■ INTRODUCTION

In recent years the need for materials with tailored properties for specific applications has led to the synthesis of polymeric nanocomposites, which frequently exhibit a combination of the properties of the individual components, although improvements can occasionally be achieved. These materials are very useful in fields where the ability to modify and control the surface wettability is highly required, such as in biotechnological applications where different surface hydrophilicity/hydrophobicity characteristics are needed,[1−7] in the investigation of protein/surface interaction necessitating the realization of surface wettability gradient,[8] and in microfluidic devices with driving flow.[9]

Versatile approaches, including appropriate external stimuli, are frequently used for the realization of smart materials with controlled and switchable surface wettability.[10,11] Light is one of the most important external stimuli,[12−14] and for this purpose several semiconductor oxides such as TiO_2, SnO_2, ZnO, and V_2O_5 are used, which increase their hydrophilicity upon UV irradiation and recover their initial wettability characteristics after dark or vacuum storage.[15−20] Recently, we presented a strategy to realize nanocomposite materials, using oleic acid-capped

titanium dioxide (TiO_2) nanorods (NRs) as nanofillers in a PMMA matrix, with tailored surface properties and reversible surface wettability. By irradiating adjacent surface areas of the films with UV light for different time intervals, we realized paths of increasing hydrophilicity, which led to directional and spontaneous water drop movement on the nanocomposites surface.[21]

Here we propose another method to modify and precisely control the surface wettability of a nanocomposite by changing the substrate and the number of photopolymerized layers realized. The photopolymerized nanocomposite films are composed of TiO_2 NRs in a polystyrene (PS) matrix, while glass and silicon are used as substrates. The substrates were chosen because of their different wettability characteristics, which strongly affect the interaction with the hydrophilic TiO_2 NRs. In particular, the NRs show a preferential interaction with the glass compared to the silicon substrates due to the higher hydrophilicity of the

former. As a consequence, when glass substrate is used, a lower number of NRs is exposed on the surface of the nanocomposite films, making them more hydrophobic than the ones prepared on silicon substrate. The situation is reversed when a second layer of nanocomposite solution is deposited over the first one and photopolymerized, since the interactions of the NRs with the underlying layer switch. By subsequent additions of successive nanocomposite layers, the wettability of the photopolymerized surface continues to swap. A detailed study of the surface morphology proves that this interesting behavior is exclusively related to the attractive or repulsive forces between the nano-composite components and the underlying surface and is in-dependent of the surface roughness, which is characterized by similar low mean values in all samples. Finally, taking advantage of the switchable wettability properties of the TiO_2 NRs upon UV irradiation,[22,23] we demonstrate the possibility to increase the initial wettability of the samples in a reversible manner using cycles of UV light and vacuum storage. The concentration of the NRs on the surface of the different samples, prepared with the layer-by-layer technique, determines the changes in the contact angle values before and after the irradiation.

■ EXPERIMENTAL SECTION

Materials. All chemicals were used as received. Styrene (ST, 99.9% purity) was purchased from Sigma-Aldrich. The photoinitiator (PI) IRGACURE 1700 (25% bis(2,6-dimethoxybenzoyl) 2,4,4-trimethylpen-tylphosphine oxide, 75% 2-hydroxy-2-methyl-1-phenylpropan-1-one (DAROCUR 1173)) was purchased from Ciba SpecialChem. The toluene solutions of oleic acid-capped TiO_2 NRs with a mean length of 20 nm and an average diameter of 3 nm was prepared as described elsewhere.[24] 1 cm × 1 cm glass microscope slides (Forlab, Carlo Erba) and bilapped polished silicon wafers (Okmetic) were used as substrates. All solvents used were purchased from Carlo Erba Reagenti.

Nanocomposite Preparation by Photopolymerization. So-lutions of ST, TiO_2 NRs, and PI in toluene were prepared so as to obtain concentrations of 94, 5, and 1 wt %, respectively. All the solutions were stirred and left under dark for several minutes to equilibrate. The first layer of the samples was prepared by spin-coating 200 μL of the above-mentioned solutions on glass or silicon substrates at 1000 rpm for 20 s. Then, to obtain the nanocomposite coating, the samples were irradiated with the third harmonic of a pulsed Nd:YAG laser (Quanta-Ray GCR-190, Spectra Physics), with an energy density of 10.5 mJ cm^{-2} (λ = 355 nm, pulse duration = 4−6 ns, repetition rate = 10 Hz) for different times depending on the substrate. For the subsequent layers, 40 μL of the above-mentioned solution was added by drop-casting onto the previously photopolymerized layer. After the photopolymerization, the samples were washed 3 times with methanol to remove unreacted monomers and PI and then dried in ambient dark condition for 2 days, in order to achieve a complete solvent evaporation. Independent experi-ments have demonstrated that after the 2 days storage period the photopolymerized samples have stable water contact angles.

Photoirradiation and Storage Processes for Reversible Wettability Changes. To enhance the hydrophilicity of the photo-polymerized nanocomposite films due to the TiO_2 NRs exposed on their surface, we irradiated the prepared films for 90 min with a pulsed Nd:YAG laser at 355 nm, (energy density of 7 mJ cm^{-2}, repetition rate of 10 Hz, pulse duration of 4−6 ns). We achieved the complete recovery of the initial wettability of the films by placing them in vacuum under dark conditions at a pressure of 3 × 10^{-3} mbar for 150 h.
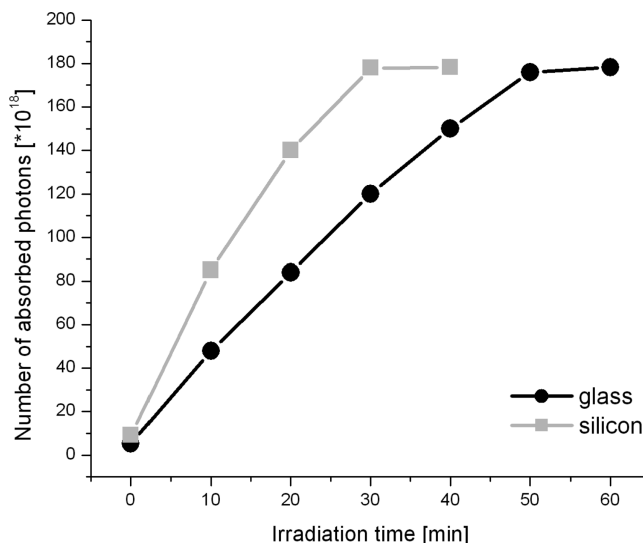

Figure 1. Comparison between the number of photons absorbed by films realized on glass and silicon substrates over time.

Characterization of Samples. Values of light transmitted through samples formed on glass and reflected by samples formed on silicon were measured using a pyroelectric joulemeter (QE25, Gentec-e).

Atomic force microscopy (AFM) study was performed for all samples using a JPK NanoWizard II system (JPK Instruments). The images were acquired in tapping mode, working in air in a vibration-insulated environment. Single-beam silicon cantilevers coated with aluminum on the reflective side (type AC160TS, Olympus), with typical elastic constant of 40 N m^{-1} and nominal tip radii of less than 10 nm, were used. The drive frequency was ~300 kHz, and the scan rate was between 0.2 and 1.0 Hz. Height was collected simultaneously with the amplitude and phase signals in both trace and retrace directions.

Adhesion force measurements were carried out in water with a JPK NanoWizard II AFM system (JPK Instruments). Soft V-shaped Si_3N_4 cantilevers with a nominal spring constant of 0.06 N m^{-1} were used (NPG, Bruker). The gold-coated AFM tips were functionalized with OH-terminated thiols (11-mercapto-1-undecanol). For each sample, the adhesion force values were obtained analyzing 400 points on four different areas.

X-ray photoelectron spectroscopy (XPS) analysis was performed to determine the chemical composition of the nanocomposite surface layers. The measurements were performed in a SPECS XRC-1000 (SPECS LAB GmbH, Berlin) system equipped with two ultrahigh-vacuum (UHV) chambers: one for sample preparation and one for sample analysis. A Mg Kα radiation source with an energy of 1253.6 eV was employed. The charge-up of binding energy (BE) values was referenced to the C1 peak at 285.6 eV as an internal standard. The number of scans and the surface of the examined samples remained the same, so that the intensity of the obtained peaks can be directly compared.

Measurements of the apparent water contact angle (WCA) were carried out with a KSV CAM200 instrument. Distilled water was used as the liquid for these tests and was dispensed using a microsyringe. The typical drop volume was around 1 μL. For each sample the contact angle value was obtained as an average of six measurements recorded on different adjacent areas of the surface.

In order to characterize the hysteresis of the samples, the advancing and receding contact angles, θ_{adv}^h and θ_{rec}^h, respectively, were mea-sured by using both the classical method, increasing and decreasing the drop volume, and by placing a water drop on the sample surface and tilting it until the droplet begins to slide. The magnitude of the
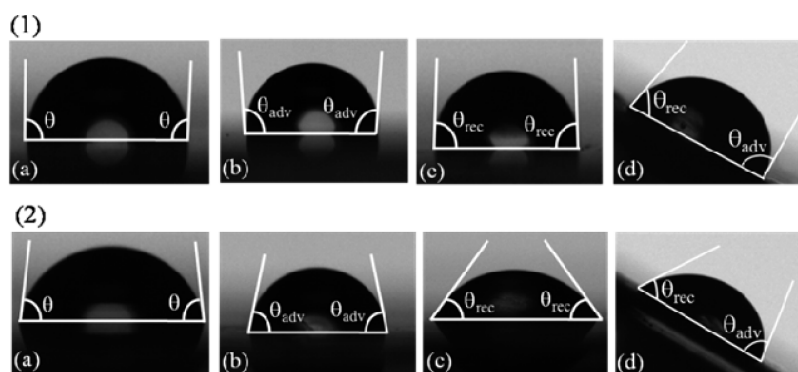
Figure 2. WCA and contact angle hysteresis measurements performed on the first layer of photopolymerized PS/TiO$_2$ NRs nanocomposite films on (1) glass and (2) silicon substrates. In all the images, frame (a) shows the apparent contact angle (θ), frame (b) shows the advancing contact angle (θ_{adv}), measured by increasing the drop volume, frame (c) shows the receding contact angle (θ_{rec}) measured by decreasing the drop volume, and frame (d) shows the drop on a tilted area, with the front contact angle being θ_{adv} and the rear contact angle being θ_{rec}. In particular, the sample on glass has an advancing contact angle of $\theta_{adv} = 97 \pm 2°$ and a receding contact angle $\theta_{rec} = 89 \pm 2°$, whereas the sample on silicon has an advancing contact angle $\theta_{adv} = 83 \pm 2°$ and a receding contact angle $\theta_{rec} = 65 \pm 2°$.

hysteresis effect ($\Delta\theta^h$) was evaluated considering the difference between the advancing and the receding contact angles, $\Delta\theta^h = \theta^h_{adv} - \theta^h_{rec}$. For this calculation, we considered the mean values of six different measurements performed on each surface, using a drop with a starting volume of 4 μL.

RESULTS AND DISCUSSION

Single-Layered Nanocomposite Films. Nanocomposite films of PS/TiO$_2$ NRs are produced by photopolymerization of homogeneous solutions of TiO$_2$ NRs in ST, deposited on different substrates. As the TEM analysis demonstrates (Supporting Information, Figure S1), the NRs stay well separated in the solutions, without forming aggregates, which would eventually lead to inhomogeneous films. The final thickness (450 $\pm$ 50 nm) of the nanocomposite films on glass and silicon substrates is obtained after 50 and 30 min of irradiation, respectively. FT-IR spectra of the photopolymerized films confirm completion of photopolymerization at the aforementioned times (Supporting Information, Figures S2 and S3). The difference in the polymerization times for samples on glass and silicon can be attributed to the different optical properties of the two substrates. In particular, the transparent glass transmits all the photons that do not react with the deposited layer, whereas the silicon reflects them, forcing them to interact again with the material. In order to verify this assumption, we estimated the number of photons absorbed by the samples deposited onto the two different substrates (Figure 1). We used the light transmitted or reflected from the samples on glass or silicon, respectively, after different irradiation times, and the analytical calculation, together with a simple model describing the photopolymerization process, is presented in the Supporting Information (Figures S4 and S5). As Figure 1 demonstrates, samples on glass and silicon absorb the same number of photons after different irradiation times. Specifically, they absorb ∼180 × 10^{18} photons at the end of their photopolymerization process, that is, after 30 min for the silicon and after 50 min for the glass, showing that the process is faster on silicon due to the reflection phenomenon. Further irradiation of the samples on both substrates does not change the number of absorbed photons, confirming that the process is terminated at the above-mentioned times.
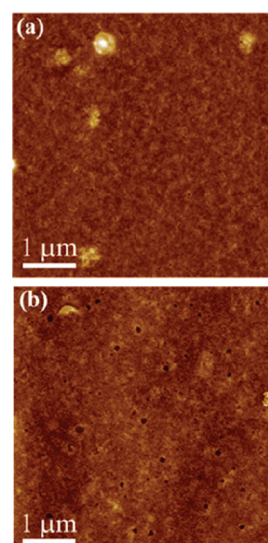

Figure 3. AFM images (height data) of the first layer of nanocomposites realized on (a) glass and (b) silicon substrate. Scan size = 5 μm, z range = 20 nm.

Apart from the different times needed for the photopolymerization of the nanocomposites onto the two different substrates, they also exhibit diverse surface wettability characteristics. Indeed, as shown in Figure 2, nanocomposite films realized on silicon (Figure 2b) are more hydrophilic (WCA = 79 $\pm$ 2°) than those prepared on glass (94 $\pm$ 2°) (Figure 2a). Moreover, as expected from the literature,[25−29] the hysteresis value of the hydrophilic samples on silicon ($\Delta\theta = 18°$) is higher than the value of the hydrophobic samples on glass ($\Delta\theta = 8°$).

The wettability of the surfaces can be affected by both the chemical composition of the material and its surface roughness. In order to justify the wettability difference between photopolymerized samples on glass and silicon, we evaluated both parameters. The AFM analysis presented in Figure 3 demonstrates that the coatings realized on the two substrates used do not show any significant differences in their topography. The mean values of their surface roughness are quite low, 1.5 $\pm$ 0.2 and 1.8 $\pm$ 0.2 nm when glass and silicon substrates are used, respectively,

almost equal considering also the experimental error. Hence, the corresponding difference in the surface roughness is too small to be associated with the wettability difference observed between the two samples.

Consequently, we assume that the wettability difference between nanocomposites on glass and on silicon can be attributed exclusively to the different chemical composition of their surface. Moreover, since the starting solution is the same, the surfaces of the prepared nanocomposites can be affected only by possible differences in the relative distribution of the solution constituents throughout the sample, eventually resulting in different percentages of TiO$_2$ NRs and polymer exposed on the films surface. These percentages for nanocomposites prepared on glass and silicon can be calculated using the following equations:

$$\%_{NRs} \times \theta_{NRs} + \%_{PS} \times \theta_{PS} = \theta_{NC} \qquad (1)$$

$$\%_{NRs} + \%_{PS} = 1 \qquad (2)$$

where $\%_{NRs}$ is the percentage of NRs and $\%_{PS}$ the percentage of PS exposed on the surface of the photopolymerized films, θ_{NRs} and θ_{PS} are the contact angles measured on films of pure TiO$_2$ and pure PS ($72 \pm 2°$ and $95 \pm 2°$, respectively, with the hydrophilic character of the NRs being attributed mainly to their surfactant-free areas), and θ_{NC} is the apparent WCA experimentally measured on the nanocomposite coatings surface. By solving the two equations, we found that the percentages of NRs exposed on the surfaces of single-layered films prepared on silicon and on glass are 69.6% and 5.0%, respectively. In order to verify that samples prepared on silicon substrates have a higher amount of NRs exposed on their surface compared to samples formed on glass substrates, we performed AFM analysis with tips functionalized with hydrophilic molecules, which interact differently with the NRs and the polymer due to the differences in their wettability. Indeed, the more hydrophilic are the examined surfaces, the larger is the adhesion force between them and the tips. For the presented surfaces, the adhesion force is lower between the tip and the polymer than between the tip and the NRs, since, as aforementioned, PS (WCA = $95 \pm 2°$) is more hydrophobic than the TiO$_2$ NRs (WCA = $72 \pm 2°$). In the histograms presented in Figure 4a, it is clearly demonstrated that the adhesion force values are higher between the AFM tips and the nanocomposites on silicon (mean force ~2.5 nN) than those between the tips and the nanocomposites on glass (mean force ~0.5 nN). Therefore, we can safely assume that a bigger number of TiO$_2$ NRs is exposed on the surface of the nanocomposite films prepared on silicon compared to those prepared on glass, supporting our previous calculations following eqs 1 and 2.

The diverse amount of NRs exposed on the surface of the nanocomposite films photopolymerized on the two substrates is further confirmed through XPS measurements. Figure 4b shows XPS peaks typical for the TiO$_2$,[30,31] i.e., the Ti 2p peak (with two components, the Ti 2p$_{1/2}$ at 465 eV and the Ti 2p$_{3/2}$ at 460 eV) and the O 1s peak (at 530 eV), in addition to the C 1s peak (at 285 eV), which could be due to the presence of both the polymer and the oleic acid surfactant of the NRs. The two presented spectra have different peak intensities due to the different number of NRs exposed on the surface of the examined samples,[30] with the peaks being higher when silicon substrate is used, indicating a bigger TiO$_2$ NRs quantity on these samples surface compared to samples prepared on glass.
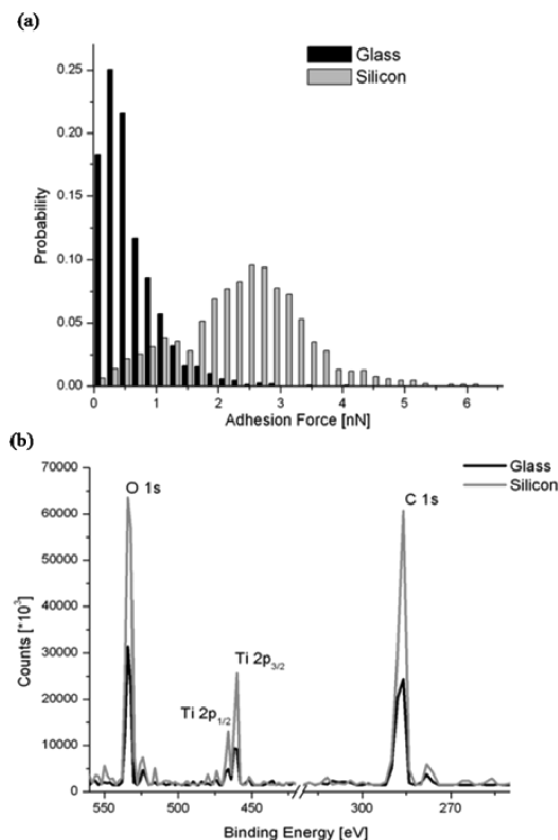

Figure 4. (a) Adhesion force peaks distribution in single-layered photopolymerized PS/TiO$_2$ nanocomposites on silicon and glass substrates. (b) Normalized XPS spectra of single-layered photopolymerized PS/TiO$_2$ samples on glass and silicon substrates, showing different peaks intensities due to the diverse surface composition.

To explain the variation in the surface content of TiO$_2$ NRs between films prepared on glass and those prepared on silicon, we consider the different hydrophilicity of the two substrates. In particular, the WCA values measured on our substrates are $40 \pm 1°$ for glass and $80 \pm 1°$ for silicon.[32] Since, as already mentioned above, the TiO$_2$ NRs have a more hydrophilic character than the ST, they are expected to interact better, through hydrophilic forces, with glass than with silicon. As a consequence, the NRs tend to move far from the silicon substrate toward the samples surface, whereas they stay close to the glass substrate due to the higher chemical affinity. The result is that a higher amount of NRs is exposed on the nanocomposites surface when they are prepared on silicon than when they are prepared on glass, and thus, water drops experience smaller contact angles and stronger adhesion in the former case than in the latter, as demonstrated by our experimental findings.

Double-Layered Nanocomposite Films. The casting of extra ST/PI/TiO$_2$ solution onto the previously photopolymerized layer, and its subsequent photopolymerization, either on glass or silicon substrate, creates a double-layered film of total thickness 950 ± 50 nm after extra 50 and 30 min of UV irradiation, respectively. The second layer shows reversed wetting characteristics with respect to the first layer. Indeed, as demonstrated in Figure 5, the double-layered films on glass have WCA of $82 \pm 2°$, lower than the one measured on the corresponding films on silicon ($93 \pm 2°$). Interestingly, the WCA of the double-layered
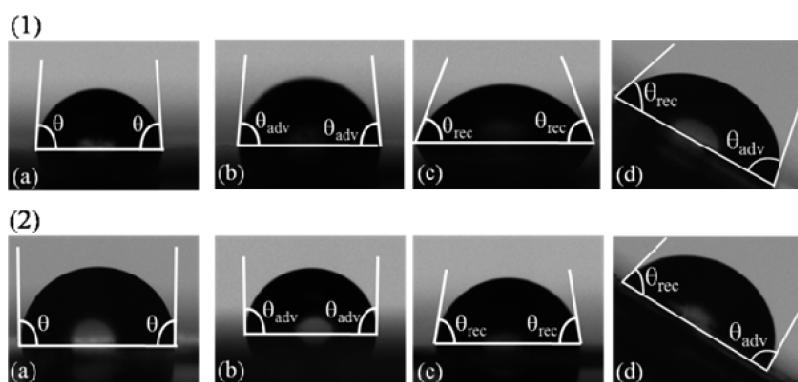
Figure 5. WCA and contact angle hysteresis measurements performed on the second layer of photopolymerized PS/TiO$_2$ NRs nanocomposite films on (1) glass and (2) silicon substrates. In all the images, frame (a) shows the apparent contact angle (θ), frame (b) shows the advancing contact angle (θ_{adv}), measured by increasing the drop volume, frame (c) shows the receding contact angle (θ_{rec}) measured by decreasing the drop volume, and frame (d) shows the drop on a tilted area, with the front contact angle being θ_{adv} and the rear contact angle being θ_{rec}. In particular, the sample on glass has an advancing contact angle $\theta_{adv} = 85 \pm 2°$ and a receding contact angle $\theta_{rec} = 67 \pm 2°$, whereas the sample on silicon has an advancing contact angle $\theta_{adv} = 95 \pm 2°$ and a receding contact angle $\theta_{rec} = 88 \pm 2°$.

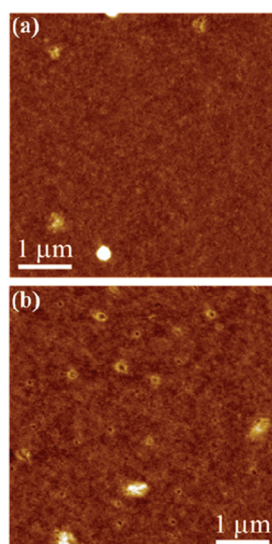**Figure 6.** AFM images (height data) of double-layered samples realized on (a) glass and (b) silicon substrate. Scan size = 5 μm, z range = 20 nm.

Figure 7. (a) Adhesion force peaks distribution in double-layered photopolymerized PS/TiO$_2$ on silicon and glass substrates. (b) Normalized XPS spectra of double-layered photopolymerized PS/TiO$_2$ on glass and silicon substrates showing different peaks intensities due to diverse surface composition.

films on glass is very similar to the one of the single-layered films on silicon, whereas the WCA of the double-layered films on silicon is very close to the one of the single-layered films on glass. As expected,[25−29] the hysteresis value of the more hydrophilic samples on glass is higher ($\Delta\theta = 18°$) than the value of the more hydrophobic samples on silicon ($\Delta\theta = 7°$), and they are both similar, but reversed, compared to the values found for the single-layered samples. To explain the different wetting characteristics between the double-layered samples on glass and silicon, we examined their topography and their chemical composition, as already presented for the single-layered samples.

The AFM topography study (Figure 6) demonstrates that the surface roughness is identical and very low for all double-layered samples, independently of their substrates (the mean values are 1.7 ± 0.2 and 1.6 ± 0.2 nm for samples on glass and silicon substrates, respectively), excluding the possibility to associate it with the surface wettability differences shown in Figure 5. Therefore, as for the single-layered nanocomposites, we can
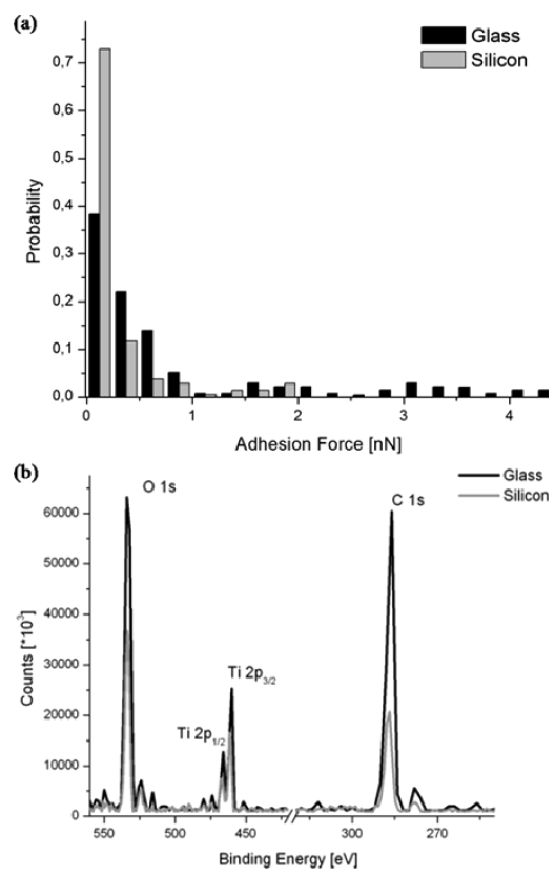
safely assume that the wettability and hysteresis differences between double-layered nanocomposites on glass and on silicon can be attributed exclusively to the different content of TiO$_2$ NRs on their surface. By using eqs 1 and 2, we calculated that the percentages of NRs exposed on the surface
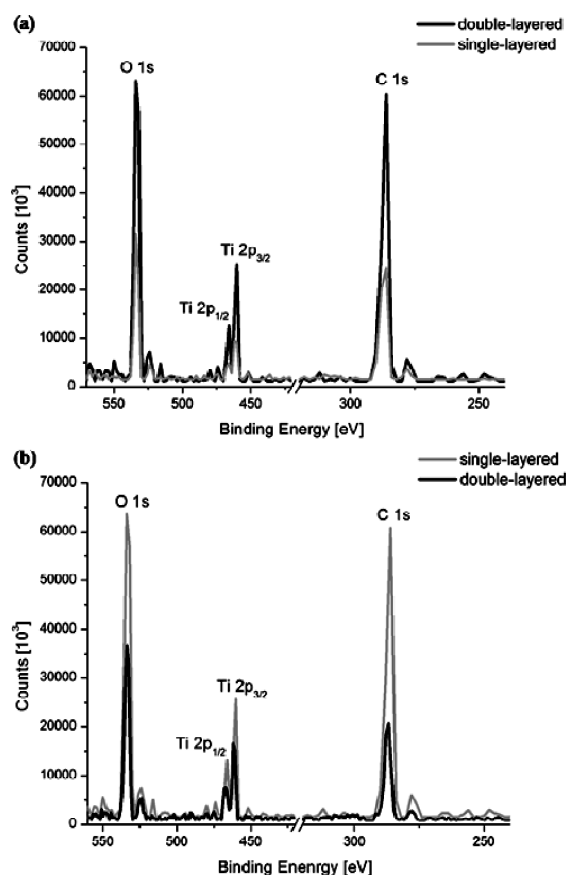
Figure 8. Normalized XPS spectra of single-layered and double-layered photopolymerized PS/TiO$_2$ samples on (a) glass and (b) silicon substrates.

Figure 9. Adhesion force peaks distribution in (a) sextuple-layered and (b) septuple-layered photopolymerized PS/TiO$_2$ films realized on both glass and silicon substrate.

of double-layered samples on silicon and glass are 9.1% and 56.5%, respectively.

The above-mentioned calculations are supported by AFM measurements performed with functionalized hydrophilic tips. The histograms in Figure 7a demonstrate that the adhesion forces between the double-layered nanocomposites and the AFM tips are higher for the samples on glass than for the samples on silicon substrates, verifying the increased hydrophilic character of the former compared to the latter. Therefore, for the reasons analyzed above, we can safely assume that a bigger number of TiO$_2$ NRs floats on the surface of the double-layered films when they are prepared on glass than when they are prepared on silicon. This assumption is further supported by the XPS measurements presented in Figure 7b, since the Ti 2p and O 1s peaks, characteristic for TiO$_2$, have increased intensity for double-layered samples prepared on glass compared to those prepared on silicon.

The increased number of TiO$_2$ NRs exposed onto the surface of the double-layered films prepared on glass with respect to those prepared on silicon can be explained by assuming hydrophilic interactions between the NRs of the second deposited layer and those on the first photopolymerized one. Therefore, considering the silicon substrate, the hydrophilic NRs of the second layer migrate close to the underlying hydrophilic layer due to increased attraction, leaving the styrene molecules exposed on the surface. For the same reason, the hydrophilic NRs float toward the surface when the second layer is deposited onto the hydrophobic first layer photopolymerized on glass.
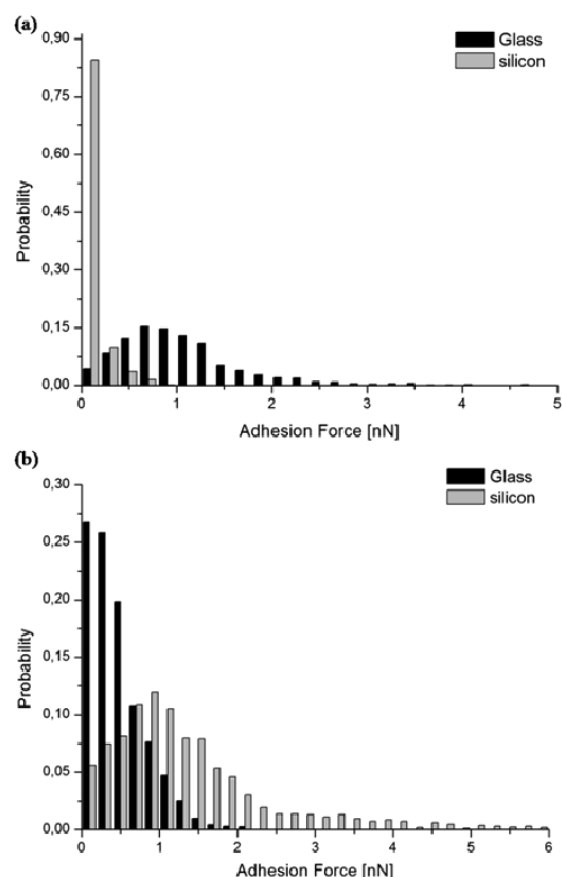
Finally, the comparison between XPS signals obtained from single-layered and double-layered samples realized on the same substrate are shown in Figure 8. This direct comparison demonstrates that the intensity of the characteristic TiO$_2$ peaks and, thus, the TiO$_2$ NRs concentration are smaller for the single-layered nanocomposites compared to the double-layered ones when they are prepared on glass, and the opposite when they are prepared on silicon, confirming the swapping in the wettability behavior of the films after the addition of the second layer.

Multilayered Nanocomposite Films. The wettability swapping demonstrated above between the first and the second layer of the nanocomposites continues as the number of photopolymerized layers realized is increased. In particular, odd-layered samples demonstrate the same surface properties as single-layered ones, and even-layered samples show the same wettability properties as double-layered ones. In confirmation of this assumption, we present samples with six and seven photopolymerized layers of PS/TiO$_2$ NRs nanocomposite, on both silicon and glass substrates. WCA measurements confirm that the sextuple-layered samples, exactly as the double-layered ones, are more hydrophobic when realized on silicon (WCA = 94 ± 2°) than when realized on glass (WCA = 81 ± 2°). On the contrary, the septuple-layered samples, as the single-layered ones, are more hydrophilic when realized on silicon (WCA = 80 ± 2°) than when realized on glass (WCA = 93 ± 2°), even though all of them show the same low roughness mean values (Supporting Information, Figures S6 and S7). The adhesion force values,
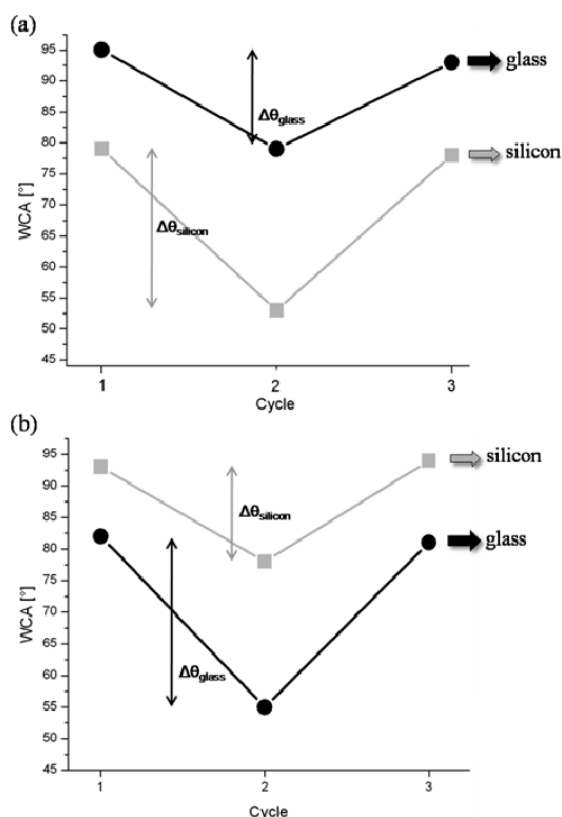
Figure 10. WCA measurements performed on (a) single-layered and (b) double-layered samples of photopolymerized PS/TiO$_2$ NRs films on silicon (■) and glass substrates (●) (1) 48 h after their photopolymerization, (2) after subsequent UV laser irradiation for 90 min, and (3) after 150 h of vacuum storage.

extracted from AFM measurements with hydrophilic functionalized tips and shown in Figure 9, confirm that sextuple-layered samples realized on glass are more hydrophilic and, thus, have higher force values compared to sextuple-layered samples formed on glass (Figure 9a), whereas septuple-layered samples on silicon have a higher hydrophilicity, and force adhesion values, compared to septuple-layered samples formed on glass (Figure 9b).

The presented "wettability swap" can be achieved exclusively by photopolymerization of successively deposited layers. Indeed, experiments conducted with solution of as-received PS polymer with NRs in toluene deposited by spin-coating on glass and silicon substrates show that the contact angle does not change with the realization of successive layers.

UV-Induced Reversible Wettability Changes. In the nanoscale, exactly as in the macroscale, TiO$_2$ demonstrates the attractive and extensively studied property of hydrophilicity increase upon UV irradiation.[33−36] Briefly, this behavior is due to the oxygen vacancies that are created on the TiO$_2$ surface upon UV irradiation, resulting into the conversion of Ti^{4+} into Ti^{3+} sites.[36] These sites are favorable for dissociative adsorption of atmospheric water molecules, leading to the formation of a highly hydroxylated (hence hydrophilic) surface.[36] This procedure is reversible,[34,36] since upon long-term storage (few months) under ambient dark conditions, or for an accelerated process, under vacuum, the adsorbed hydroxyl groups can be removed and eventually replaced by ambient oxygen, allowing the initial wettability

to be recovered. Since, as demonstrated above, an odd number of nanocomposite layers photopolymerized on silicon and an even number of nanocomposite layers photopolymerized on glass have increased TiO$_2$ NRs content on their surface, the phenomenon of UV-induced increased hydrophilicity is expected to be enhanced for the specific samples. As a representative example, we present the results for single- and double-layered samples. Indeed, Figure 10a shows the WCA decrease for single-layered samples on silicon and glass (step 2) after UV laser irradiation for 90 min. This decrease is higher for the samples on silicon, with the difference in WCA being $\Delta WCA = 26°$ (WCA after UV becomes $53 \pm 2°$), compared to the decrease for the samples on glass, which is $\Delta WCA = 14°$ (WCA after UV becomes $79 \pm 2°$). As expected, the higher WCA decrease of the samples realized on silicon substrates is due to the higher number of the surface-exposed NRs. Analogously, the hydrophilic character of the double-layered systems is enhanced upon UV laser irradiation, more for samples on glass than for samples on silicon (Figure 10b). Indeed, the UV-induced change (step 2) of the WCA is $\Delta WCA = 27°$ for glass (postirradiation WCA = $55 \pm 2°$) and $\Delta WCA = 17°$ for silicon (postirradiation WCA = $78 \pm 2°$). The initial wettability of all samples is fully recovered after their storage in vacuum for 150 h, and the demonstration for single- and double-layered coatings is shown in step 3 of Figure 10a,b.

The accurate control of the change in the wetting properties of the formed surfaces using UV laser irradiation, together with the ability of defining the initial WCA of the films, can be essential for the development of multifunctional devices, for microfluidics, or for biological molecules and cells attachment and growth, avoiding the use of complicated instrumentation and expensive substrates and materials.

■ CONCLUSIONS

We demonstrated a strategy to realize nanocomposite films with tailored surface properties using photopolymerization of solutions of styrene, photoinitiator, and TiO$_2$ nanorods on different substrates. It was found that all the examined films have similar and low surface roughness and that the nanorods distribution on the surface, and, thus, the surface wettability of the resulting materials, depends exclusively on the interaction of the nanorods with the underlying substrate. Specifically, it was found that the first nanocomposite layer prepared on silicon demonstrates a higher hydrophilicity compared to that prepared on glass. With the addition of a second layer the wettability of the films is reversed, resulting in films with a higher hydrophilicity when formed on glass compared to those formed on silicon. Successive additions of photopolymerizable layers continue to swap the wettability characteristics. These systems show a reversible change in their hydrophilicity upon UV irradiation and vacuum storage cycles, with the magnitude of these changes accurately defined by the number of nanorods exposed on the samples surface, demonstrating, thus, an increased wettability change when a higher amount of nanorods is exposed on the films surface. The successful and easy realization of patterned nanocomposite films with tunable and highly controlled wettability characteristics, using two commonly exploited substrates, versatile nanoparticles and widely commercially available monomers, opens up the way for the incorporation of these nanocomposites into specific parts of systems and devices, such as cell growth systems,[37−39] microfluidic devices,[21] etc.

■ ASSOCIATED CONTENT

ⓢ Supporting Information. Figure S1, showing a TEM image of the ST/PI/TiO$_2$ solution before photopolymerization; Figures S2 and S3, showing FT-IR spectra of photopolymerized and as-received PS/TiO$_2$ NRs samples, respectively; Figure S4, showing a schematic representation of the light measurements; Figure S5, showing a simple model of the photopolymerization process; Figure S6, showing the WCA values of sextuple- and septuple-layered samples, both on glass and silicon substrate; and Figure S7, showing AFM images of sextuple- and septuple-layered samples on glass and silicon substrates. This material is available free of charge via the Internet at http://pubs.acs.org.

■ AUTHOR INFORMATION

Corresponding Author

*E-mail: francesca.villafiorita@unisalento.it (F.V.-M.); athanassia.athanassiou@iit.it (A.A.).

■ ACKNOWLEDGMENT

■ REFERENCES

(1) Janczuk, B.; Zdziennicka, A. *J. Mater. Sci.* **1994**, *29*, 3559–3564.

(2) Kwok, S. C. H.; Wang, J.; Chu, P. K. *Diamond Relat. Mater.* **2005**, *14*, 78–85.

(3) Zhang, S.; Du, H.; Ong, S. E.; Aung, K. N.; Too, H. C.; Miao, X. *Thin Solid Films* **2006**, *515*, 66–72.

(4) Barhoumi, H.; Maaref, A.; Jaffrezic-Renault, N. *Langmuir* **2010**, *26*, 7165–7173.

(5) Hanifah, S. A.; Heng, L. Y.; Ahmad, S. *Anal. Sci.* **2009**, *25*, 779–784.

(6) Reetz, M. T.; Zonta, A.; Simpelkamp, J.; Rufinska, A.; Tesche, B. *J. Sol-Gel Sci. Technol.* **1996**, *7*, 35–43.

(7) Menaa, B.; Herrero, M.; Rives, V.; Lavrenko, M.; Eggers, D. K. *Biomaterials* **2008**, *29*, 2710–2718.

(8) Elwing, H.; Welin, S.; Askendal, A.; Nilsson, U.; Lundstrom, I. *J. Colloid Interface Sci.* **1987**, *119*, 203–210.

(9) Grunze, M. *Science* **1999**, *283*, 41–42.

(10) Feng, X.; Jiang, L. *Adv. Mater.* **2006**, *18*, 3063–3078.

(11) Gras, S. L.; Mahmud, T.; Rosengarten, G.; Mitchell, A.; Kalantar-zadeh, K. *ChemPhysChem* **2007**, *8*, 2036–2050.

(12) Wang, S.; Song, Y.; Jiang, L. *J. Photochem. Photobiol., C* **2007**, *8*, 18–29.

(13) Athanassiou, A.; Lygeraki, M. I.; Pisignano, D.; Lakiotaki, K.; Varda, M.; Mele, E.; Fotakis, C.; Cingolani, R.; Anastasiadis, S. H. *Langmuir* **2006**, *22*, 2329–2333.

(14) Athanassiou, A.; Varda, M.; Mele, E.; Lygeraki, M. I.; Pisignano, D.; Farsari, M.; Fotakis, C.; Cingolani, R.; Anastasiadis, S. H. *Appl. Phys. A: Mater. Sci. Process.* **2006**, *83*, 351–356.

(15) Borras, A.; Barranco, A.; Gonzalez-Elipe, A. R. *Langmuir* **2008**, *24*, 8021–8026.

(16) Hou, W.; Wang, Q. *Langmuir* **2009**, *25*, 6875–6879.

(17) Zhang, X. T.; Jin, M.; Liu, Z. Y.; Tryk, D. A.; Nishimoto, S.; Murakami, T.; Fujishima, A. *J. Phys. Chem. C* **2007**, *111*, 14521–14529.

(18) Liu, H.; Feng, L.; Zhai, J.; Jiang, L.; Zhu, D. B. *Langmuir* **2004**, *20*, 5659–5661.

(19) Caputo, G.; Cortese, B.; Nobile, C.; Salerno, M.; Cingolani, R.; Gigli, G.; Cozzoli, P. D.; Athanassiou, A. *Adv. Funct. Mater.* **2009**, *19*, 1149–1157.

(20) Caputo, G.; Cingolani, R.; Cozzoli, P. D.; Athanassiou, A. *Phys. Chem. Chem. Phys.* **2009**, *11*, 3692–3700.

(21) Villafiorita Monteleone, F.; Caputo, G.; Canale, C.; Cozzoli, P. D.; Cingolani, R.; Fragouli, D.; Athanassiou, A. *Langmuir* **2010**, *26*, 18557–18563.

(22) Feng, X.; Zhai, J.; Jiang, L. *Angew. Chem., Int. Ed.* **2005**, *44*, 5115–5118.

(23) Wang, D.; Liu, Y.; Liu, X.; Zhou, F.; Liua, W.; Xuea, Q. *Chem. Commun.* **2009**, *45*, 7018–7020.

(24) Cozzoli, P. D.; Kornowski, A.; Weller, H. *J. Am. Chem. Soc.* **2003**, *125*, 14539–14548.

(25) Bormashenko, E.; Bormashenko, Y.; Whyman, G.; Pogreb, R.; Musin, A.; Jager, R.; Barkay, Z. *Langmuir* **2008**, *24*, 4020–4025.

(26) Lai, Y.-H.; Yang, J.-T.; Shieh, D.-B. *Lab Chip* **2010**, *10*, 499–504.

(27) Nosaka, A.; Fujiwara, T.; Yagi, H.; Akutsu, H.; Nosaka, Y. *J. Phys. Chem. B* **2004**, *108*, 9121–9125.

(28) Zhao, H.; Beysens, D. *Langmuir* **1995**, *11*, 627.

(29) Moumen, N.; Subramanian, R. S.; McLaughlin, J. B. *Langmuir* **2006**, *22*, 2682–2690.

(30) Erdem, B.; Hunsicker, R. A.; Simmons, G. W.; Sudol, E. D.; Dimonie, V. L.; El-Aasser, M. S. *Langmuir* **2001**, *17*, 2664–2669.

(31) McCafferty, E.; Wightman, J. P. *Surf. Interface Anal.* **1998**, *26*, 549–564.

(32) Franssila, S. *Introduction to Microfabrication*; John Wiley & Sons, Ltd.: New York, 2004.

(33) Caputo, G.; Cortese, B.; Nobile, C.; Salerno, M.; Cingolani, R.; Gigli, G.; Cozzoli, P. D.; Athanassiou, A. *Adv. Funct. Mater.* **2009**, *19*, 1149–1157.

(34) Caputo, G.; Cingolani, R.; Cozzoli, P. D.; Athanassiou, A. *Phys. Chem. Chem. Phys.* **2009**, *11*, 3692–3700.

(35) Caputo, G.; Nobile, C.; Buonsanti, R.; Kipp, T.; Manna, L.; Cingolani, R.; Cozzoli, P. D.; Athanassiou, A. *J. Mater. Sci.* **2008**, *43*, 3474–3480.

(36) Caputo, G.; Nobile, C.; Kipp, T.; Blasi, L.; Grillo, V.; Carlino, E.; Manna, L.; Cingolani, R.; Cozzoli, P. D.; Athanassiou, A. *J. Phys. Chem. C* **2008**, *112*, 701–714.

(37) Zhao, L.; Mei, S.; Wang, W.; Chu, P. K.; Wu, Z.; Zhang, Y. *Biomaterials* **2010**, *31*, 2055–2063.

(38) Laroussi, M.; Leipold, F. *Int. J. Mass Spectrom.* **2004**, *233*, 81–86.

(39) Sato, T. *Appl. Phys. Lett.* **2006**, *89*, 073902 (2 pages).

■ NOTE ADDED AFTER ASAP PUBLICATION

This article was published ASAP on June 3, 2011. Changes were made to the author's affiliation addresses. The corrected version was posted on June 9, 2011.